



# Impact of future aircraft NO<sub>x</sub> emissions on atmospheric composition and climate: dependence on background conditions

Zosia Staniaszek<sup>1</sup>, Didier A. Hauglustaine<sup>2</sup>, Yann Cohen<sup>2,3</sup>, Agnieszka Skowron<sup>4</sup>, Sigrun Matthes<sup>5</sup>, Robin Thor<sup>5</sup>, Marianne T. Lund<sup>1</sup>

<sup>1</sup>Center for International Climate and Environmental Research (CICERO), Oslo, 0349, Norway

<sup>2</sup>Laboratoire des Sciences du Climat et de l'Environnement, LSCE-IPSL (CEA–CNRS–UVSQ), Université Paris-Saclay, 91191 Gif-sur-Yvette, France

<sup>3</sup>Institut Pierre-Simon Laplace, Sorbonne Université/CNRS, Paris, France

<sup>4</sup>Faculty of Science and Engineering, Manchester Metropolitan University, Manchester, M1 5GD, United Kingdom

<sup>5</sup>Institut für Physik der Atmosphäre, Deutsches Zentrum für Luft und Raumfahrt, Oberpfaffenhofen, Germany

*Correspondence to:* Zosia Staniaszek (zosia.staniaszek@cicero.oslo.no)

## Abstract

Aviation emissions are predicted to have caused 4% of anthropogenic warming to date. While aviation CO<sub>2</sub> climate effects are well known, the magnitude of non-CO<sub>2</sub> effects of aviation are highly uncertain. Nitrogen oxide (NO<sub>x</sub>) emissions from aircraft affect greenhouse gases: local production of ozone in the short term, and long-term impacts on methane, stratospheric water vapour and ozone. Ozone production is non-linear and depends on the background concentrations of NO<sub>x</sub> and volatile organic compounds (VOCs). Previous single-model studies have found an increased sensitivity of NO<sub>x</sub>-induced response to aviation emissions in high-mitigation scenarios compared to low-mitigation scenarios. Here we extend this to a multi-model study, using three models to explore the dependence of aviation NO<sub>x</sub> effects on background conditions in two future scenarios. We calculate the ozone radiative forcing from a 20% change in aviation NO<sub>x</sub> emissions for two different future aviation emission scenarios, running each scenario in a high and low mitigation background. We do not find a consistent sensitivity of ozone response to NO<sub>x</sub> background between the models used. The inter-model variability in ozone response is larger than the effect of different background scenarios. We calculate a positive net NO<sub>x</sub> forcing in both future scenarios; in the high mitigation scenario in two of three models the long-term methane forcing is sufficiently negative to make the net NO<sub>x</sub> forcing negative. There is continued uncertainty in the climate impacts of aviation NO<sub>x</sub>, and we suggest that more model consensus is required to enable parametrisations of these NO<sub>x</sub> impacts into simplified models.



## 1 Introduction

30 The aviation sector contributes around 3% of annual carbon dioxide (CO<sub>2</sub>) emissions globally (IEA, 2025). Non-CO<sub>2</sub> emissions from aviation exert both direct and indirect effects on climate, and are estimated to have double the impact on climate until present compared to CO<sub>2</sub> from aviation (Lee et al., 2021). These non-CO<sub>2</sub> emissions include aerosols, water vapour and nitrogen oxides (NO<sub>x</sub>). NO<sub>x</sub> emissions in turn lead to impacts on tropospheric ozone formation in the short term, and reduce methane concentrations and lifetime via hydroxyl radical (OH) reactions (Fuglestad et al., 1999). Both methane and ozone

35 are key short-lived climate forcers, and the resulting methane changes also affect ozone on a long-term (5-10 year) scale, as well as stratospheric water vapour, which also has a radiative impact. Overall, emissions from aviation are estimated to have caused 4% of anthropogenic global warming to date, and a corresponding projected 0.1 degree of warming by 2050 (Aamaas et al., 2025; Klöwer et al., 2021). Non-CO<sub>2</sub> impacts contribute around 8 times more uncertainty than CO<sub>2</sub> in the estimates of aviation's climate impact (for 2018, Lee et al. 2021).

40 The impacts of aviation on climate from CO<sub>2</sub> are well known – CO<sub>2</sub> is a long-lived greenhouse gas, and emissions of CO<sub>2</sub> from aircraft have a global warming impact that is independent of emissions location and time of day. By contrast, the non-CO<sub>2</sub> impacts of aviation on climate have a much higher uncertainty associated with them due to the many processes involved, including cloud and contrail formation, direct and indirect aerosol effects, and non-linear ozone chemistry (Righi et al., 2021; Burkhardt & Kärcher, 2011; Myhre et al., 2011; Gettelman & Chen, 2013; Groöß et al., 1998). The formation of ozone is

45 strongly dependent on the background levels of both NO<sub>x</sub> and volatile organic compounds (VOCs), so the impact of a perturbation in NO<sub>x</sub> emissions (such as from aviation) on ozone depends on the local chemical composition of NO<sub>x</sub> and VOCs. The ozone production efficiency is location and season dependent, for example with increased efficiency of ozone production from NO<sub>x</sub> released at higher cruise altitudes (Søvde et al., 2014; Terrenoire et al., 2022). Several previous studies have explored the sensitivity of the ozone response to aviation NO<sub>x</sub> in different atmospheric backgrounds. More polluted sites are

50 less sensitive to the addition of more NO<sub>x</sub>, with the most important control being background NO<sub>x</sub> levels (Stevenson & Derwent, 2009; Holmes et al., 2011). This means that the response to aviation NO<sub>x</sub> is dependent on the regional and vertical distribution of the emissions (Köhler et al., 2008a; Lund et al., 2017). Increased lightning NO<sub>x</sub> emissions (and therefore background NO<sub>x</sub>) have been found to lead to a reduction in the aviation-induced ozone perturbation (Khodayari et al., 2018). The net aviation NO<sub>x</sub> response includes long-term changes in methane, ozone and stratospheric water vapour, which are also

55 affected by the background atmospheric composition, due to differences in the atmospheric oxidising capacity. More recently, using the revised formula for calculating methane radiative forcing from Etminan et al. (2016) has led to a stronger estimated negative methane forcing from aviation NO<sub>x</sub>, which may outweigh the ozone forcing, resulting in a negative net NO<sub>x</sub> forcing under certain conditions (Skowron et al., 2021; Terrenoire et al., 2022). Skowron et al. (2021) found that the aviation net NO<sub>x</sub> forcing was lower in high mitigation (low NO<sub>x</sub>) scenarios, and that this was particularly dependent on background surface

60 NO<sub>x</sub> emissions, with any 1% change in surface NO<sub>x</sub> emissions modifying aircraft net NO<sub>x</sub> RF by ~1.5%. The short-term ozone and methane responses have different sensitivities to the background conditions, and the net response depends on the



balance between them (Skowron et al., 2021; Stevenson & Derwent, 2009). Many of these studies use a single model, and there is a need for multi-model studies on the net impact of aviation NO<sub>x</sub> (Terrenoire et al., 2022).

Chemistry-climate models (CCMs) and chemistry-transport models (CTMs) are used to quantify climate impacts of aviation and probe different scenarios. Due to model differences in chemistry, transport and parametrisations of the processes involved, there is high model spread in the predicted climate impact of aviation, especially for non-CO<sub>2</sub> impacts (Holmes et al., 2011; Lee et al., 2021; Olsen et al., 2013). Therefore, multi-model studies with comparable scenarios and experimental setup are required to further understand and explain these differences, as part of the path forward for reducing the uncertainty of non-CO<sub>2</sub> aviation impacts. Here we use MOZART3, LMDZ-INCA, OsloCTM3 and EMAC models to explore the climate impacts of aviation NO<sub>x</sub> (Hauglustaine et al., 2004; Kinnison et al., 2007; Pozzer et al., 2011; Søvde et al., 2012). This work is closely related to two previous studies focusing on the climatology of these models and comparison with observations (Cohen et al., 2024), and the present-day impact of aviation NO<sub>x</sub> and aerosols (Cohen et al., 2025b). We expand on these to consider future scenarios and the influence of different background atmospheric conditions.

Future pathways for the aviation sector span a wide range of possibilities combining changes in demand, regional distribution, new technologies aimed at decarbonisation, and more (ICAO, 2025, Aamaas et al. 2025). The Shared Socioeconomic Pathways (SSPs) from the sixth Coupled Model Intercomparison Project (CMIP6) span this range: SSP3-7.0 is characterised by unabated increases in air pollution, slow implementation of new technologies, and increasing aviation demand, while SSP1-2.6 includes strong air pollution reduction measures, emphasis on low-carbon technologies, and limited increases in air traffic (Fujimori et al., 2017; Gidden et al., 2019; van Vuuren et al., 2017). The future impacts of aviation on climate depend both on the aviation emissions trajectory, and the background emissions (Skowron et al., 2021; Hodnebrog et al., 2011), so it is crucial to assess if these non-linearities in the NO<sub>x</sub>-induced ozone production can be confirmed in a multi-model study.

For this purpose, we explore the short-term ozone and overall impacts of aviation NO<sub>x</sub> emissions, in the present day and for the SSP1-2.6 and SSP3-7.0 future scenarios in 2050. The next section outlines the experiments performed and models used, section 3 compares the short-term ozone climate impact of aviation in the future and present day, and section 4 explores the sensitivity of this effect to background conditions in the different SSPs.

## 2 Methods

We show results from a multi-model study of global chemistry and climate models (CCMs and GCMs, section 2.1). We explore the changes in atmospheric ozone distribution and net radiative forcing (section 2.2) induced by aviation NO<sub>x</sub> emissions, and the sensitivity of these to the background state.

### 2.1 Multi-model experiments

The numerical experiments in this multi-model study were carried out under the European Union project ‘Advancing the Science for Aviation and Climate’ (ACACIA). Six models participated, four of which ran the future aviation experiments



95 **Table 1: Model description overview for global atmospheric models used in this study. First column abbreviations horiz., vert., hom., phot., and het. correspond respectively to: horizontal, vertical, homogenous, photolytic and heterogeneous. Aerosol categories include sulfate (SO<sub>4</sub>), nitrate (NO<sub>3</sub>), black carbon (BC) and organic carbon (OC).**

<b>Model</b>	<b>MOZART3</b>	<b>LMDZ-INCA</b>	<b>OsloCTM3</b>	<b>EMAC</b>
Institution (user)	MMU	LSCE (IPSL)	CICERO	DLR
Model type	CTM	CCM (CTM mode)	CTM	CCM (CTM mode)
Reanalysis	ERA-Interim	ERA5	ECMWF OpenIFS	ERA-Interim
GCM	–	LMDZ	–	ECHAM5
Horiz. resolution	2.8°E x 2.8°N	2.5°E x 1.3°N	2.25°E x 2.25°N	2.8°E x 2.8°N
Vertical levels	60	39	60	90
Vert. resolution (hPa) near cruise levels	20–30	25–40	25–30	15–20
Top level (hPa)	0.10	0.012	0.10	0.010
<b>Chemistry</b>				
Total species	108	174	190	160
Aerosol species	–	26	56	–
Hom. reactions	218	390	263	265
Phot. reactions	71	80	61	82
Het. reactions	18	39	18	12
Aerosol categories	–	SO <sub>4</sub> , NO <sub>3</sub> , NH <sub>4</sub> , BC, OC, dust, sea-salt	SO <sub>4</sub> , NO <sub>3</sub> , NH <sub>4</sub> , BC, OC, SOA, dust, sea-salt	–
<b>Emissions</b>				
Lightning	Price et al. 1997, Pickering et al. 1998	Price and Rind 1992, Ott et al. 2010	Price and Rind 1992, Ott et al. 2010	Grewe et al. 2001
Biogenic VOCs	POET	ORCHIDEE model	MEGAN-MACC	
Biomass burning	BB4CMIP	BB4CMIP	GFED4	

studied here: MOZART3 (Kinnison et al., 2007), LMDZ-INCA (Hauglustaine et al., 2004, 2014), OsloCTM3 (Søvde et al., 2012) and EMAC (Pozzer et al., 2011). Table 1 shows a comparison of the setup, chemistry and emissions of these models. For a full description of the models, and evaluation of model differences in atmospheric composition compared to observations, see Cohen et al., (2024).

100 This study focuses on aviation-induced effects associated with NO<sub>x</sub> emissions in future scenarios, exploring the influence of different background conditions. Table 2 outlines the relevant experiments performed as part of the wider multi-model study. Perturbations of -20% for NO<sub>x</sub> aviation emissions were implemented in a present-day (2014-2018) scenario and for two future scenarios in 2050 (SSP1-2.6 and SSP3-7.0, hereafter referred to as SSP1 and SSP3) (Gidden et al., 2019). To test the sensitivity of the ozone response to different background conditions, both future emissions scenarios were run with SSP1 and SSP3  
 105 backgrounds. The experiments are all timeslice runs, with present-day meteorology, run for four years, with the average of the last three years used for analysis. The present-day emissions are from the Community Earth atmospheric Data System (CEDS) inventory (Hoesly et al., 2018), and the SSP1 and SSP3 emissions (including aviation scenarios and long-lived greenhouse gases) are from CMIP6 (Gidden et al., 2019). We use the corrected CEDS aviation emissions from (Thor et al., 2023). In section 3, to compare the impact attributable to the aviation sector in present and future we use results from the -20%  
 110 perturbations (Air-20 scenarios) and scale them up to 100% to give a whole sector estimate e.g. (Köhler et al., 2008b). We use model-specific scaling factors from the PD\_Air-20 and equivalent -100% experiments from Cohen et. al 2025b, which range between 1.09 and 1.18. For EMAC, the PD\_Air-20 experiment was not performed, so we use the -100% experiment directly. For the sensitivity analysis (section 4) the results are all from the -20% experiments.

115 **Table 2: Simulations from the ACACIA projects used in this study, performed by models MOZART3, LMDZ-INCA, OsloCTM3 and EMAC (present day and SSP3 only, for the latter). Background refers to all non-aviation emissions and chemical state. NO<sub>x</sub> aviation emissions were perturbed by 20% compared to the baseline (present day, SSP1 and SSP3). LMDZ-INCA reductions include aerosols and NO<sub>x</sub>.**

Label	Background	Aviation Emissions	Description
REF_PD	2014–2018	2014–2018	Present Day (PD)
PD_Air-20	2014–2018	2014–2018 - 20%	PD - 20% aviation NO <sub>x</sub> emissions
REF_SSP1	SSP1	SSP1	SSP1 baseline
SSP1_Air-20	SSP1	SSP1-20%	SSP1 - 20% aviation NO <sub>x</sub> emissions
REF_SSP3BG_SSP1Air	SSP3	SSP1	SSP1 baseline with SSP3 background
SSP3BG_SSP1Air-20	SSP3	SSP1-20%	As above - 20% aviation NO <sub>x</sub> emissions
REF_SSP3	SSP3	SSP3	SSP3 baseline
SSP3_Air-20	SSP3	SSP3-20%	SSP3 - 20% aviation NO <sub>x</sub> emissions
REF_SSP1BG_SSP3Air	SSP1	SSP3	SSP3 baseline with SSP1 background
SSP1BG_SSP3Air-20	SSP1	SSP3 - 20%	As above – 20% aviation NO <sub>x</sub> emissions

Here we use a perturbation method, where we compare experiments with 20% lower aviation emissions with a baseline experiment (REF\_PD, REF\_SSP1 or REF\_SSP3). This contrasts to source apportionment methods, where pollutants are tagged and their transport and reaction pathways are tracked. These two methods give different results due to the non-linearity of the NO<sub>x</sub>-O<sub>3</sub> system. (Maruhashi et al., 2024) compared these methods and found a factor of 1.16 to 2.55 difference between the tagging and perturbation methods for the ozone response to NO<sub>x</sub> emissions, with the tagging method simulating higher ozone production. For sensitivity analysis such as that done in section 4, perturbation methods are the most appropriate and this is the method we have used.

## 2.2 Radiative forcing calculations

The ozone radiative forcing (RF) was calculated from the aviation-induced ozone perturbations using a concentration-based kernel from Skeie et al (2020), which compares favourably to offline radiative transfer calculations from OsloCTM3 (Lund et al., 2021) and LMDZ-INCA (see Table S3, Cohen et al., 2025b; Terrenoire et al., 2022). 3D monthly averages of ozone mixing ratio from each model were conservatively interpolated onto a  $2.25^\circ \times 2.25^\circ$  grid and linearly interpolated in pressure onto 60 vertical levels, from the surface up to 0.1 hPa, to match the kernel grid. The ozone column (in Dobson Units, DU) was calculated using air mass from OsloCTM3 for all models, following the method in Skeie et al. (2020). From this, using the kernel (in  $\text{W m}^{-2} \text{DU}^{-1}$ ), the radiative forcing response (in  $\text{W m}^{-2}$ ) was calculated. The kernel takes into account the sensitivity of ozone RF to location (see Skeie et al., (2020) Fig S1). In some areas of the atmosphere, such as the upper free troposphere, changes in ozone produce a much stronger RF per DU impact than ozone changes at higher or lower altitudes (e.g. Köhler et al., 2008b). When aviation emissions affect ozone in these areas, this gives a greater short-term ozone climate impact per Tg of NO<sub>x</sub>.

The change in methane mixing ratio,  $\Delta CH_4$ , and the associated radiative forcing,  $RF_{CH_4}$ , are calculated based on the modelled change in methane lifetime from each simulation ( $\Delta\tau_{CH_4}$ ), combined with the methane feedback factor and an emission non-steady state factor, as shown in Equation 1 (method described in Berntsen et al., 2005; Hodnebrog et al., 2012; Terrenoire et al., 2022, Cohen et al., 2025b). The methane reference mixing ratios in 2050  $[CH_4]_{SSP}$  are taken from O'Neill et al., 2016 (i.e. 2472 ppbv for scenario SSP3-7.0 and 1519 ppbv for scenario SSP1-2.6). The methane feedback on its own lifetime ( $f_{feedback} = 1.45$ ) is taken as the model mean from a recent model intercomparison (Sand et al., 2023).  $f_{non-steady}$  is a factor to correct for the fact that due to its long lifetime methane steady state is not reached, so assuming steady-state to derive the radiative forcing overstates the response. Based on the method described by Grewe and Stenke (2008) we recalculated these factors for 2050 conditions for both SSP1-2.6 and SSP3-7.0 future scenarios and derived non-steady factors of 1.06 and 0.90 respectively.

$$\Delta CH_4 = \Delta\tau_{CH_4} \times [CH_4]_{SSP} \times f_{feedback} \times f_{non-steady} \quad (1)$$



From this methane mixing ratio change, the methane RF is calculated using the simplified equation from Etminan et al., 2016 (Equation 2).

$$RF_{CH_4} = \left[ -1.3 \cdot 10^{-6} \overline{[CH_4]} - 8.2 \cdot 10^{-6} [N_2O] + 0.043 \right] \left[ \sqrt{[CH_4]} - \sqrt{[CH_4]_{SSP}} \right] \quad (2)$$

where  $[CH_4]$  is the perturbed methane mixing ratio,  $\overline{[CH_4]}$  the mean (calculated between the perturbed and reference value) methane mixing ratio, and  $[N_2O]$  the  $N_2O$  mixing ratio in 2050 (taken to be 355 ppbv). The indirect long-term ozone and stratospheric water vapour RFs are calculated based on the change in methane mixing ratio adopting the normalized forcings from a recent model intercomparison (Sand et al., 2023). For long-term ozone we use a normalized forcing of  $0.180 \text{ W/m}^2/\text{CH}_4$  ppbv and for stratospheric water a normalized forcing of  $0.058 \text{ W/m}^2/\text{CH}_4$  ppbv. The RFs are also converted to ERF using the ERF/RF ratios from Lee et al. (2021) to give an estimate of net NOx ERF with an efficacy of 1.370 for the short-term ozone forcing and 1.180 for the methane direct and indirect forcings.

### 3 Comparison of future and present-day aviation NOx-induced effects

To provide context for the future aviation scenarios, we first compare aviation NOx emissions in the SSP1 and SSP3 scenarios to the present-day, by calculating the short-term ozone radiative forcing associated with aviation NOx emissions. Nitrogen oxides are co-emitted with greenhouse gases in combustion processes, and also affect local air quality, so NOx emissions are controlled via both climate and air quality policies. SSP1 represents an optimistic future trajectory with stringent air quality and climate policies, while SSP3 has increasing greenhouse gas and ozone precursor emissions in a rapidly warming world (Gidden et al., 2019). Figs 1a,b show the spatial distribution of the present-day aviation NOx emissions in these experiments. NOx emissions in 2050 for SSP3 are around 50% higher than the present day, while in SSP1 they are ~25% lower (see Figs 1c,d,e). The NOx emissions in the present-day, SSP1 and SSP3 scenarios are 3.78, 2.86, 5.80  $\text{TgNO}_2$  per year respectively. The spatial distribution of the NOx emissions is similar in the present day and future scenarios, due to assumptions about continuing air traffic trends in the underlying SSP scenarios. The SSP3 and SSP1 scenarios correspond to the upper and lower bounds (for  $\text{CO}_2$  emissions) in future scenarios used by the International Civil Aviation Organization up to 2070 (LTAG scenarios, Aamaas et al., 2025; ICAO, 2025), with the upper bound representing no new technologies or operational improvements, and the lower bound fixed at 2019 levels.



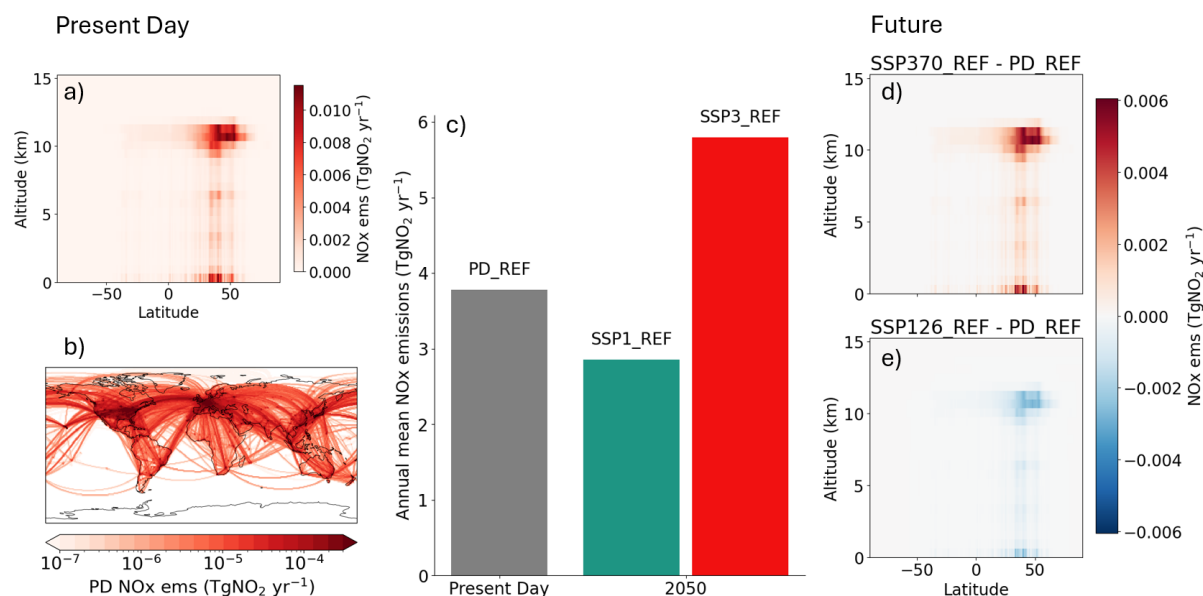


**Fig 1: NO<sub>x</sub> emissions in present-day (a,b) and future (c,d,e) scenarios, in TgNO<sub>2</sub>/yr. a) Zonal mean NO<sub>x</sub> emissions from present day. b) Global distribution in present day (whole column sum). c) Annual mean sum of emissions. d,e) Zonal mean difference between future and present-day NO<sub>x</sub> emissions for SSP1 and SSP3 respectively (compared to (a)).**

The ozone attributable to aviation NO<sub>x</sub> emissions (in the short term, not including long-term effects via methane) is shown in Fig 2a,b, for the present day and future scenarios. Fig 2a shows the total mass of ozone (burden) and Fig 2b shows the vertical distribution. The models show two grouped responses: a stronger ozone response at a higher altitude (LMDZ-INCA, MOZART3, ~200hPa), or a weaker, lower peak ozone response (EMAC and OsloCTM3, ~300hPa, see Fig 2b). The altitude of the aviation NO<sub>x</sub> emissions is consistent between models, so the differences in the vertical distribution of the ozone response, and how localised it is, are attributable to the model chemistry and atmospheric transport. Cohen et al., 2025b compared the climatology of the models used here to long-term airborne observations (IAGOS: In-service Aircraft for a Global Observing System; (Petzold et al., 2015)) in the upper troposphere and lowermost stratosphere. They found that the models overestimate and underestimate ozone concentrations in these regions respectively. Results from present-day simulations using the same model ensemble suggest that in the upper troposphere, where the NO<sub>x</sub> is emitted, photochemical production of ozone causes the short-term ozone increase, while in the lowermost stratosphere, the increase is likely a combination of less transport across the tropopause, and less ozone destruction via OH (Cohen et al. 2025). The seasonality of the ozone response varies between models, with a peak ozone response in April for EMAC, and in June for OsloCTM3 and MOZART3. There is considerable model spread in short-term ozone response to aviation NO<sub>x</sub> emissions, in terms of magnitude and seasonality of response – for more details see (Cohen et al., 2025b).



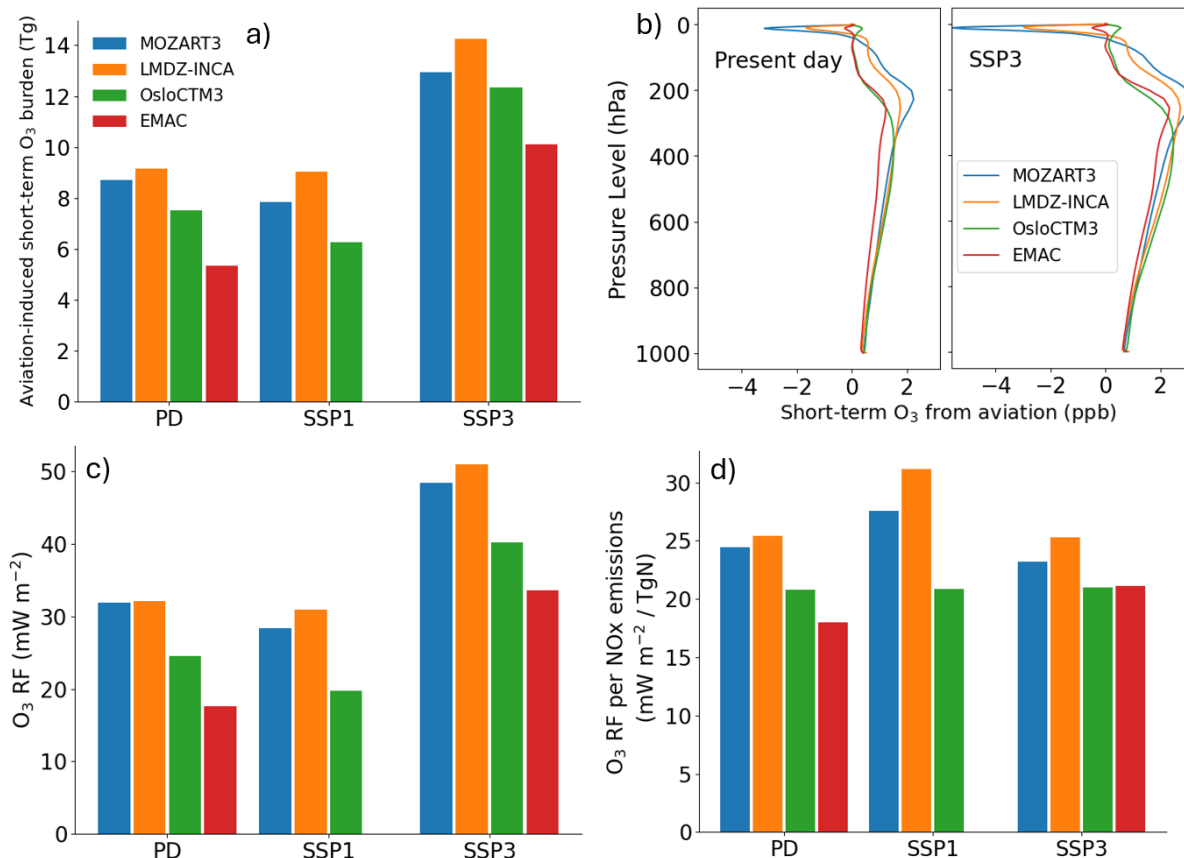


**Fig 2: Short-term ozone concentrations and radiative forcing (RF) from aviation emissions in present-day, SSP1 and SSP3 scenarios. (a) aviation induced short-term ozone burden, (b) vertical profiles of ozone mixing ratio attributed to short-term effect of aviation emissions for present-day and SSP3 (c) unscaled ozone RF and (d) ozone RF normalised by NO<sub>x</sub> emissions change.**

Fig 2c shows the radiative forcing associated with the aviation-induced ozone concentrations. The present day and SSP1 RFs are relatively similar (27 (18-32) and 26 (19-27) mW m<sup>-2</sup> respectively), compared to the higher aviation impact in SSP3 (43 (34-51) mW m<sup>-2</sup>). This is partly due to differences in aviation NO<sub>x</sub> emissions in the different scenarios, as shown in Fig 1; the aviation sector in SSP3 is larger and therefore has a greater radiative impact. Lee et al. 2021 calculated a short-term ozone RF for present day (2018) of 36.0 (23 - 56) mW m<sup>-2</sup>, based on a review of previous studies. We find a lower present-day RF, with a smaller range, and all models except EMAC are within the Lee et al. (2021) range. When normalised by the NO<sub>x</sub> emissions, the short-term ozone RFs are more comparable across the scenarios (Fig 2d). Previous studies have shown a higher sensitivity of ozone to NO<sub>x</sub> emissions changes in high-mitigation scenarios (like SSP1) compared to other scenarios (e.g. Skowron et al. (2021)), which we see for two of the three models (MOZART3 and LMDZ-INCA). Here, the inter-model differences in ozone response to NO<sub>x</sub> emissions are larger than the inter-scenario differences (see Fig 2d). We explore this sensitivity further in the next section.



#### 4 Sensitivity of the aviation impacts to background conditions

215 We use paired experiments with the same aviation emissions, but different background conditions (SSP1 and SSP3, see Fig 1) to look at the sensitivity of the short-term ozone response to background state. Only models that ran the SSP1BG\_SSP3Air (and SSP3BG\_SSP1Air, see Table 2) are included in this analysis (i.e. excluding EMAC). Ozone production is determined non-linearly by NO<sub>x</sub> concentrations, VOC concentrations, temperature and sunlight, and so the short-term ozone response to changes in NO<sub>x</sub> emissions is expected to be dependent on the location of emissions and the local chemical state. Skowron et al., (2021) found that the short-term ozone RF from aviation emissions depended on the background NO<sub>x</sub> conditions, including surface NO<sub>x</sub> concentrations.

We use the SSP experiments in Table 2, with 20% reductions in aviation emissions (for SSP1 and SSP3 emissions), in an SSP1 and SSP3 background. Fig 3 shows the global mean short-term ozone RF impact of these emissions, with colours representing different models, and hatching/dotted lines showing results from an SSP1 background. We find a range of model responses to changes in background. MOZART3 simulates very similar global ozone RF with SSP1 and SSP3 backgrounds, i.e. the RF is found to be independent of the background in these experiments. In OsloCTM3, an SSP1 background yields a lower ozone RF (lower sensitivity of ozone to NO<sub>x</sub> emissions) and LMDZ-INCA shows the opposite effect, with a larger short-term ozone RF in an SSP1 background. Skowron et al. 2021 also used MOZART3, with different background scenarios (RCPs) and different emissions scenarios (2.2 and 5.6 TgN/yr), with a 100% perturbation in aviation emissions, resulting in a significantly larger perturbation than this study, and found a strong sensitivity of NO<sub>x</sub> response to the background conditions. MOZART3 has the highest non-linearity in ozone response of the three models used here (Table S2, Cohen et al. 2025b).

For all models here, the sensitivity to background was the same sign for both SSP1 and SSP3 emissions scenarios: higher in SSP1BG for LMDZ-INCA, lower in SSP1BG for OsloCTM3 and similar for both backgrounds in MOZART3. These changes in RF for the different models in varying backgrounds are consistent with the underlying change in ozone column (Fig 3c compared to Fig3a). Fig 3b shows the vertical distribution of the change in short-term ozone RF. This shows some of the model diversity in response to the same NO<sub>x</sub> emissions change, with e.g. MOZART3 giving a more localized, higher altitude response and OsloCTM3 showing a lower altitude and more vertically distributed ozone response. Overall, the inter-model differences in ozone RF response are larger than the response to a change in background state.

The global sum of short-term ozone radiative forcing masks heterogeneity in the underlying ozone response in different areas of the atmosphere. The three models show a different response in terms of where the ozone impact is the largest. This is largely due to differences in model chemistry and transport, as the magnitude and location of aviation NO<sub>x</sub> emissions were consistent between models, but there may be small differences due to different model vertical pressure grids and therefore injection heights (Terrenoire et al., 2022). Fig 4 shows the zonal mean differences in (a) ozone mixing ratio (b) and ozone (short-term) RF between the SSP1 background and the SSP3 background (SSP1 – SSP3), for the SSP3 emissions experiment. The corresponding figures for the SSP1 emissions experiment are shown in Fig S2. An increase (red) means that an SSP1

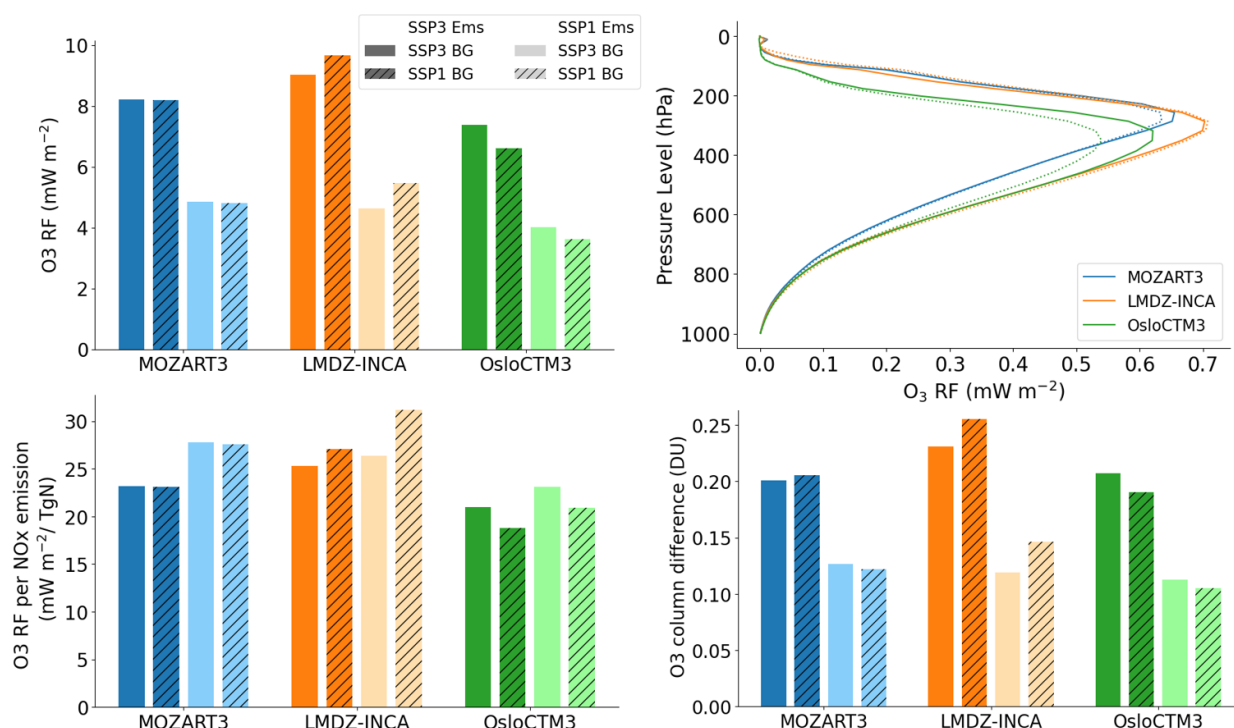


**Fig 3: Short-term ozone radiative forcing for a 20% reduction in aviation emissions for SSP1 and SSP3 (darker and lighter colours respectively) with varying background emissions (SSP3 solid and SSP1 hatched). (a) ozone RF global sum, (b) vertical profile of ozone RF, solid line is SSP3 emissions and background, dotted line is SSP3 emissions with SSP1 background.**

background gives a higher ozone concentration or RF, i.e. a higher ozone sensitivity. Figs 4c and 4d show the vertical difference in short-term ozone RF (SSP1BG – SSP3BG) for SSP3 and SSP1 emissions respectively.

The models all show lower ozone concentrations in the northern mid latitude upper troposphere, and higher concentrations in the lowermost stratosphere, under an SSP1 background compared to an SSP3 background (Fig 4a), although the relative magnitude of these changes varies between models, giving a different net response. In MOZART3, lower net ozone production in the NOx emissions region (in SSP1BG compared to SSP3BG), and higher net ozone production elsewhere leads to no net difference due to the background (Fig 4a,b left panels). All models also show an increased ozone response in SSP1 compared to SSP3 in the northern hemisphere lower levels, which may contribute to air pollution, especially in scenarios where surface air pollutant concentrations are low (E.g. SSP1).

Due to differences in model chemistry and transport, given the same surface VOC and NOx emissions, the models simulate different background conditions for the upper troposphere lower stratosphere (UTLS) region (see Fig S4), which is important for the aviation NOx response. For MOZART3, the UTLS background is similar in SSP1 and SSP3, suggesting that what drives the ozone response are the aircraft emissions and non-linearities. LMDZ-INCA simulates lower NOx concentrations in the UTLS region in the SSP1 background, while OsloCTM3 shows slightly higher NOx concentration in SSP1 (Fig S4). This is consistent with a higher and lower sensitivity, respectively, in the ozone response to aviation NOx emissions in the UTLS

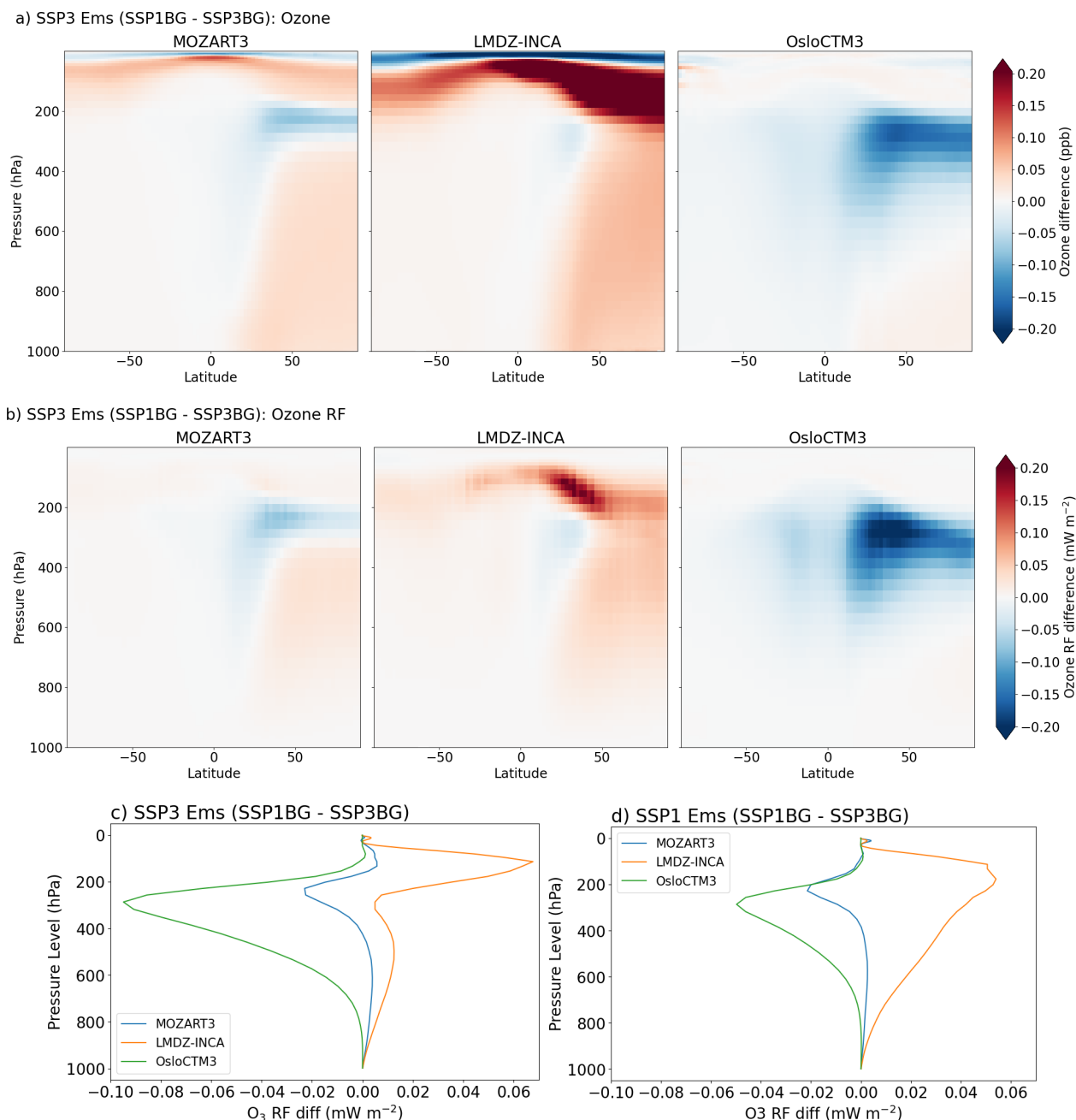


**Fig 4: Difference between (a) ozone mixing ratio change and (b) ozone RF for a 20% reduction in SSP1 and SSP3 backgrounds. Positive (red) means that there is greater ozone reduction in SSP1 than in SSP3 background, i.e. higher sensitivity. Vertical profile of difference in ozone RF in SSP1 background compared to SSP3 background for c) SSP3 emissions and d) SSP1 emissions.**



275

280

285

290

295

300

region. From Cohen et al., 2025b, we know that LMDZ-INCA transports aviation emissions to the UTLS region leading to accumulation there, and a higher background response. OsloCTM3 and MOZART3 do not show this strong positive response in the UTLS region, which may be due to more similar background NO<sub>x</sub> in the UTLS region in SSP1 and SSP3, and/or due to less transport of the emissions to this region. The larger spatial differences in ozone concentration response (Fig 4a) are modulated by the radiative forcing kernel, due to the spatial heterogeneity of RF sensitivity, which is largest in the upper free troposphere (Skeie et al., 2020). This means that the model diversity in ozone RF response (Fig 4b) is smaller than the diversity in ozone mixing ratio response (Fig 4a). In terms of vertical profiles, the SSP1 emissions experiment gives a smaller ozone RF response, due to lower initial aviation emissions. Again, the models are internally consistent between experiments, but show different signs for the response to an SSP1 background.

The sensitivities we find here contrast to previous model studies, for example Skowron et al. (2021) also used MOZART3 and found a strong sensitivity of short-term ozone change to background and surface NO<sub>x</sub>. LMDZ-INCA shows a strong ozone increase at higher altitudes, in the lowermost stratosphere (and MOZART3 and OsloCTM3 to a much lesser extent). This suggests that in LMDZ-INCA, a larger amount of aviation NO<sub>x</sub> from the perturbation reaches the lowermost stratosphere, where the local chemical environment is more sensitive to NO<sub>x</sub> injection, and means a small perturbation in NO<sub>x</sub> emissions leads to more ozone destruction (Köhler et al., 2008b; Maruhashi et al., 2024). To quantify the ozone sensitivity to NO<sub>x</sub> emissions we calculate the change in ozone burden per change in NO<sub>x</sub> emissions ( $\text{TgO}_3 / (\text{TgN yr}^{-1})$ , Fig S3). Since consistent emissions were used between models, the sensitivity is consistent with the results shown in Fig 3: LMDZ-INCA shows a higher sensitivity in an SSP1 background, OsloCTM3 lower, and MOZART3 gives mixed results, with an ensemble mean of 7.2 (5.9-9.1)  $\text{Tg O}_3 / (\text{TgN yr}^{-1})$ .

Fig 1 shows the similar spatial distribution of aviation emissions in the present-day and both future scenarios. Different regional distributions of future aviation NO<sub>x</sub> emissions, given different potential scenarios for evolution of the aviation sector, are not represented in the SSP scenarios. The future scenarios used here (and available in the literature) are therefore a limited representation of the whole scope of future emissions and impacts. A shift in aviation patterns (for example towards the Global South) would lead to a different regional distribution of aviation emissions, and would likely impact sensitivity to background conditions (Maruhashi et al., 2024). Here we do not take into account changes in underlying climate: changes in temperature and humidity, which affect reaction rates and oxidant concentrations, combined with different background NO<sub>x</sub> and VOC emissions would affect ozone production and therefore the aviation NO<sub>x</sub> impact (e.g. Griffiths et al., 2021).

#### 4.1 Net NO<sub>x</sub> radiative forcing

We calculate the methane, long-term ozone and stratospheric water vapour RFs to give a net NO<sub>x</sub> RF corresponding to the aviation sector in the future scenarios. Previous studies have shown that in some cases with high-mitigation background scenario (similar to SSP1), the negative methane component of the RF becomes larger, and enough to make the net NO<sub>x</sub> RF negative (Skowron et al., 2021; Terrenoire et al., 2022). Fig 5 shows the net NO<sub>x</sub> RFs calculated for these experiments as

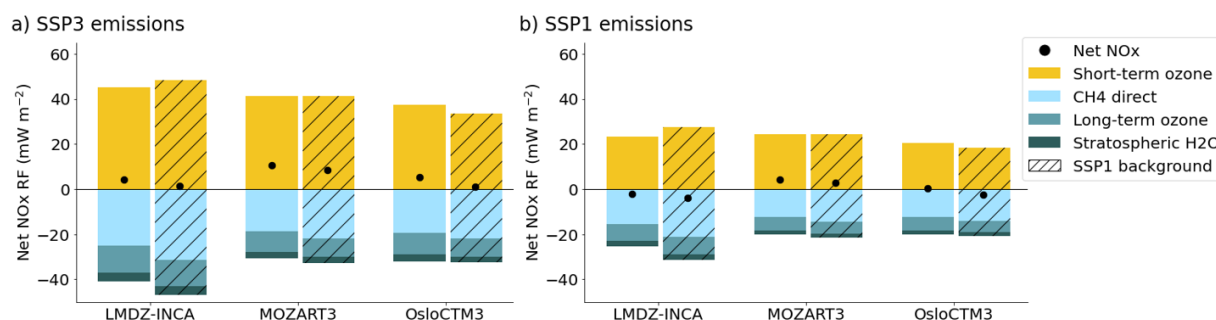


**Fig 5: Net NO<sub>x</sub> Radiative Forcing (RF) calculated from 20% reductions in aviation emissions in a) SSP3 and b) SSP1 scenarios, with SSP3 (solid) and SSP1 (hatched) background emissions. The net NO<sub>x</sub> RF comprises short-term and long-term ozone, methane and stratospheric water vapour. Data for all components is available in Table S1.**

outlined in section 2.2, with hatching showing the SSP1 background experiments. We do not find a consistent sign change in net NO<sub>x</sub> RF with a change in background, although the methane RF component is larger in all of the SSP1 background experiments, and causes the net NO<sub>x</sub> forcing to be negative in LMDZ-INCA and OsloCTM3 for SSP1 emissions. For OsloCTM3, this means that although the short-term ozone response is weaker in an SSP1 background, the methane lifetime response is larger. In LMDZ-INCA the net NO<sub>x</sub> forcing is negative for SSP1 emissions regardless of background. We find a global, model mean net NO<sub>x</sub> forcing for aviation emissions in SSP3 of  $6.7 \text{ mW m}^{-2}$  (4.1-10.6, multi-model range) and in SSP1 of  $-1.2 \text{ mW m}^{-2}$  (-3.8 - 2.7). The net NO<sub>x</sub> RF for the corresponding present-day experiments is  $8.5 \pm 3.5 \text{ mW m}^{-2}$  (5 models, Cohen et al., 2025b). Lee et al (2021) calculated a net NO<sub>x</sub> RF of  $8.2 \text{ mW m}^{-2}$  (-4.8 - 16)  $\text{mW m}^{-2}$  for 2018 emissions, which when scaled to the NO<sub>x</sub> emissions used here corresponds to  $10.2 \text{ mW m}^{-2}$ , consistent with our multi-model range. We also calculate the net NO<sub>x</sub> ERFs to enable comparison with other studies (see Table S2). To do this, we use the ERF/RF ratios from Lee et al., (2021), with a caveat that due to absence of better information, these are assumed to be equal to efficacy factors from a single study and are therefore associated with a high uncertainty (Ponater et al., 2006).

The use of 2014–2018 meteorology here means that the effects of future climate change are not included, as discussed in the previous section, and which has been highlighted as an ongoing question (Terrenoire et al., 2022). There is high uncertainty in the trajectories of future aviation emissions, both in terms of magnitude and spatial distribution (Aamaas et al., 2025). This depends on changes in technology, adoption of low-carbon fuels and changing regional demand. The resulting changes in the latitudinal distribution of NO<sub>x</sub> emissions could lead to differences in the sensitivity of the ozone response to aviation emissions, for example if the shift leads to more aviation emissions in previously low-NO<sub>x</sub> regions.

A steady state factor (1.06 for SSP1 and 0.90 for SSP3) is used in the RF calculations to account for the fact that methane cannot respond interactively in these models, since the lower boundary condition is set at the surface. Performing the RF calculation without this steady-state factor gives a net negative forcing in all scenarios for LMDZ-INCA and for the SSP1 background scenarios for OsloCTM3, while the MOZART3 net NO<sub>x</sub> RFs remain positive with and without the steady state scaling factor. This highlights the importance of the methane contribution and the potential for it to result in a net negative NO<sub>x</sub> RF, as emphasised by Skowron et al. (2021) who did not use a steady state factor. Here, the methane RF (and therefore



net NO<sub>x</sub> RF) is sensitive to the value used for the steady state factor, which has a high uncertainty and scenario dependence. This is a limitation from using models with a lower boundary condition for methane, rather than an interactive scheme where the methane mixing ratio can respond to NO<sub>x</sub>, OH and ozone changes over time (e.g. Folberth et al., 2022).

The net NO<sub>x</sub> estimates here do not account for changes in aerosols resulting from aviation NO<sub>x</sub> emissions. Prashanth et al., 2022 estimated that aviation NO<sub>x</sub> causes -3.4 mWm<sup>-2</sup> of secondary aerosol forcing, via nitrate and sulfate aerosols. Terrenoire et al. (2022) found that the inclusion of this nitrate and sulfate forcing could change the sign of the net NO<sub>x</sub> RF from positive to negative. The secondary aerosol impacts are strongly dependent on the NH<sub>3</sub> and SO<sub>2</sub> levels in the upper troposphere, and are therefore strongly affected by background scenario. Unger et al. 2013) found a superlinear response in nitrate aerosol forcing to aviation NO<sub>x</sub>, with 4x and 10x larger forcing in 2050 compared to present day, for a low and high mitigation scenario respectively. In the present-day experiments using the same models as in this study, Cohen et al. (2025b) found very high model diversity in present-day aerosol responses to aviation, based on the complexity of the aerosol scheme used.

## 5 Conclusions

We use an ensemble of models (LMDZ-INCA, MOZART3, EMAC and OsloCTM3) to evaluate the impact of aviation NO<sub>x</sub> emissions on climate in future scenarios, with SSP1 and SSP3 background states to probe the sensitivity of short-term ozone response to background conditions. We find a multi-model mean short-term ozone radiative forcing from aviation of 41.3 (37.4 - 45.2) mWm<sup>-2</sup> in SSP3 and 23.3 (18.4 - 27.4) mWm<sup>-2</sup> in SSP1 for the future scenarios, compared to 27 (18 - 32) mW m<sup>-2</sup> in present day. The differences are largely attributable to the differences in aviation NO<sub>x</sub> emissions between these scenarios. When scaled to NO<sub>x</sub> emissions, the short-term ozone forcing per NO<sub>x</sub> emission is 23 (21 - 25), 27 (21 - 31) and 22 (18 - 25) mW m<sup>-2</sup> / TgN for SSP3, SSP1 and PD respectively. The higher sensitivity in SSP1 compared to SSP3 and present day is driven by LMDZ-INCA and MOZART3, while OsloCTM3 shows the same sensitivity regardless of scenario (see Fig 2d). We find a large model spread in ozone response to aviation NO<sub>x</sub>: inter-model differences in ozone response in any given scenario are greater than the differences between scenarios.

When comparing experiments with the same emissions but different backgrounds (SSP1 and SSP3) directly, we do not find model agreement on the sensitivity of the ozone radiative forcing to changes in background (NO<sub>x</sub> and VOC emissions, and methane concentrations). LMDZ-INCA shows the expected response, with increased sensitivity to emissions in a cleaner (SSP1) background, OsloCTM3 shows the reverse response and MOZART3 shows little sensitivity to background conditions. There is model diversity in the in upper troposphere/lower stratosphere background response to different emissions scenarios, or how effectively surface emissions affect this region in the different models. This has an impact on the sensitivity of the aviation NO<sub>x</sub>-induced ozone response to different backgrounds. We do not find agreement with previous single model studies that show strong background dependence of aviation impacts – when considered in a multi-model approach, these results are inconclusive. This suggests that more work is needed in this area to quantify the sensitivity of the aviation NO<sub>x</sub> impact to





different backgrounds, which has wide applications e.g. in simple climate models and in the aviation sector for planning non-CO<sub>2</sub> mitigation measures. For example, Aamaas et al., (2025) (using a parameterization of NO<sub>x</sub> dependence on background  
370 based on Skowron et al., (2021)) simulate a 0.06 °C spread in aviation NO<sub>x</sub>-induced global mean surface temperature (GMST) change based on different background scenarios, of a total aviation-induced GMST increase between 2020 and 2070 of 0.15 °C under a high aviation emission scenario. The parametrisation of the background dependence of the NO<sub>x</sub> response is dependent on model results, for which we find no consensus with these three models. An improved understanding of NO<sub>x</sub>-induced effects is particularly relevant for the development of operational mitigation strategies, e.g. contrail avoidance by  
375 flying higher or lower, as the ozone response to NO<sub>x</sub> is highly altitude dependent. These measures may lead to adverse impacts from aviation NO<sub>x</sub> in the future, and may change the sensitivity of ozone response to background conditions.

We estimate the net radiative forcing from aviation NO<sub>x</sub> by including the effects of long-term changes in ozone, stratospheric water vapour and methane. We find a positive net NO<sub>x</sub> radiative forcing for the aviation experiments under both SSP1 and  
380 SSP3 future emissions scenarios with an SSP3 background (except LMDZ-INCA with SSP1 emissions). When switching to an SSP1 background, the negative forcing from methane gives a sufficiently negative long-term forcing to counteract the positive short-term ozone forcing in OsloCTM3 and LMDZ-INCA, consistent with previous studies (Skowron et al., 2021). Our derivation of the methane mixing ratio response from the change in lifetime, including the use of a steady-state factor, is a limitation on the methane forcing estimate, and increases its uncertainty. The use of methane boundary conditions as standard  
385 in CCMs and CTMs limits a fully interactive methane response. The quantification of aviation NO<sub>x</sub> forcing in methane emissions-driven models, including sensitivity to background, would be key in improving the understanding of aviation NO<sub>x</sub> impacts.

### Code and data availability

Model data from the relevant experiments used in this study can be accessed at <https://zenodo.org/records/16949722> (Cohen  
390 et al., 2025a). Scripts for analysis and making figures in this paper and the Supplement can be found at [https://github.com/zosiast/ACACIA\\_future\\_paper3\\_figs](https://github.com/zosiast/ACACIA_future_paper3_figs).

### Author Contributions

All authors contributed to the conceptualisation of the study. MTL, YC, AS and RT carried out the model experiments. ZS and DH performed the analysis. ZS prepared the manuscript, with contributions from all co-authors.



## 395 Competing Interests

The authors declare that they have no conflict of interest.

## Acknowledgements

This research has been funded by the European Union Horizon 2020 Research and Innovation programme, within the framework of the ACACIA (grant agreement no. 875036) project.

## 400 References

- Aamaas, B., Lund, M. T., Fuglestedt, J. S., Totterdill, A., Owen, B., Skowron, A., & Lee, D. S. (2025). Continued global warming from aviation even under high-ambition mitigation scenarios. *One Earth*, 0(0).  
<https://doi.org/10.1016/j.oneear.2025.101451>
- Berntsen, T. K., Fuglestedt, J. S., Joshi, M. M., Shine, K. P., Stuber, N., Ponater, M., Sausen, R., Hauglustaine, D. A., & Li, L. (2005). Response of climate to regional emissions of ozone precursors: Sensitivities and warming potentials. *Tellus B: Chemical and Physical Meteorology*, 57(4), 283–304. <https://doi.org/10.3402/tellusb.v57i4.16549>
- Burkhardt, U., & Kärcher, B. (2011). Global radiative forcing from contrail cirrus. *Nature Climate Change*, 1(1), 54–58.  
<https://doi.org/10.1038/nclimate1068>
- Cohen, Y., Hauglustaine, D., Bellouin, N., Lund, M. T., Matthes, S., Skowron, A., Thor, R., Bundke, U., Petzold, A., Rohs, S., Thouret, V., Zahn, A., & Ziereis, H. (2024). *Multi-model assessment of climatologies in the upper troposphere–lower stratosphere using the IAGOS data*. Gases/Atmospheric Modelling and Data Analysis/Troposphere/Chemistry (chemical composition and reactions). <https://doi.org/10.5194/egusphere-2024-2208>
- Cohen, Y., Hauglustaine, D., Lund, M. T., Skowron, A., Matthes, S., & Thor, R. (2025a). *Perturbation simulations for aircraft NO<sub>x</sub> and aerosol emissions in present day and future: Multi-model data from the ACACIA EU project* [Dataset]. Zenodo. <https://doi.org/10.5281/ZENODO.16949721>
- Cohen, Y., Hauglustaine, D., Staniaszek, Z., Lund, M. T., Dedoussi, I., Matthes, S., Quadros, F., Righi, M., Skowron, A., & Thor, R. (2025b). Impact of present aircraft NO<sub>x</sub> and aerosol emissions on atmospheric composition and climate: Results from a model intercomparison. *EGUsphere*, 1–43. <https://doi.org/10.5194/egusphere-2025-4273>



- Etminan, M., Myhre, G., Highwood, E. J., & Shine, K. P. (2016). Radiative forcing of carbon dioxide, methane, and nitrous  
 420 oxide: A significant revision of the methane radiative forcing. *Geophysical Research Letters*, 43(24), 12,614–12,623.  
<https://doi.org/10.1002/2016GL071930>
- Folberth, G. A., Staniaszek, Z., Archibald, A. T., Gedney, N., Griffiths, P. T., Jones, C. D., O'Connor, F. M., Parker, R. J.,  
 Sellar, A. A., & Wiltshire, A. (2022). Description and Evaluation of an Emission-Driven and Fully Coupled Methane  
 Cycle in UKESM1. *Journal of Advances in Modeling Earth Systems*, 14(7), e2021MS002982.  
 425 <https://doi.org/10.1029/2021MS002982>
- Fuglestad, J. S., Berntsen, T. K., Isaksen, I. S. A., Mao, H., Liang, X.-Z., & Wang, W.-C. (1999). Climatic forcing of nitrogen  
 oxides through changes in tropospheric ozone and methane; global 3D model studies. *Atmospheric Environment*,  
 33(6), 961–977. [https://doi.org/10.1016/S1352-2310\(98\)00217-9](https://doi.org/10.1016/S1352-2310(98)00217-9)
- Fujimori, S., Hasegawa, T., Masui, T., Takahashi, K., Herran, D. S., Dai, H., Hijioka, Y., & Kainuma, M. (2017). SSP3: AIM  
 430 implementation of Shared Socioeconomic Pathways. *Global Environmental Change*, 42, 268–283.  
<https://doi.org/10.1016/j.gloenvcha.2016.06.009>
- Gottelman, A., & Chen, C. (2013). The climate impact of aviation aerosols. *Geophysical Research Letters*, 40(11), 2785–2789.  
<https://doi.org/10.1002/grl.50520>
- Gidden, M. J., Riahi, K., Smith, S. J., Fujimori, S., Luderer, G., Kriegler, E., van Vuuren, D. P., van den Berg, M., Feng, L.,  
 435 Klein, D., Calvin, K., Doelman, J. C., Frank, S., Fricko, O., Harmsen, M., Hasegawa, T., Havlik, P., Hilaire, J.,  
 Hoesly, R., ... Takahashi, K. (2019). Global emissions pathways under different socioeconomic scenarios for use in  
 CMIP6: A dataset of harmonized emissions trajectories through the end of the century. *Geoscientific Model  
 Development*, 12(4), 1443–1475. <https://doi.org/10.5194/gmd-12-1443-2019>
- Grewe, V., & Stenke, A. (2008). AirClim: An efficient tool for climate evaluation of aircraft technology. *Atmospheric  
 440 Chemistry and Physics*, 8(16), 4621–4639. <https://doi.org/10.5194/acp-8-4621-2008>
- Griffiths, P. T., Murray, L. T., Zeng, G., Shin, Y. M., Abraham, N. L., Archibald, A. T., Deushi, M., Emmons, L. K., Galbally,  
 I. E., Hassler, B., Horowitz, L. W., Keeble, J., Liu, J., Moeini, O., Naik, V., O'Connor, F. M., Oshima, N., Tarasick,



- D., Tilmes, S., ... Zanis, P. (2021). Tropospheric ozone in CMIP6 simulations. *Atmospheric Chemistry and Physics*, 21(5), 4187–4218. <https://doi.org/10.5194/acp-21-4187-2021>
- 445 Groöß, J., Brühl, C., & Peter, T. (1998). Impact of aircraft emissions on tropospheric and stratospheric ozone. Part I: Chemistry and 2-D model results. *Atmospheric Environment*, 32(18), 3173–3184. [https://doi.org/10.1016/S1352-2310\(98\)00016-8](https://doi.org/10.1016/S1352-2310(98)00016-8)
- Hauglustaine, D. A., Balkanski, Y., & Schulz, M. (2014). A global model simulation of present and future nitrate aerosols and their direct radiative forcing of climate. *Atmospheric Chemistry and Physics*, 14(20), 11031–11063. <https://doi.org/10.5194/acp-14-11031-2014>
- 450 Hauglustaine, D. A., Hourdin, F., Jourdain, L., Filiberti, M.-A., Walters, S., Lamarque, J.-F., & Holland, E. A. (2004). Interactive chemistry in the Laboratoire de Météorologie Dynamique general circulation model: Description and background tropospheric chemistry evaluation. *Journal of Geophysical Research: Atmospheres*, 109(D4). <https://doi.org/10.1029/2003JD003957>
- 455 Hodnebrog, Ø., Berntsen, T. K., Dessens, O., Gauss, M., Grewe, V., Isaksen, I. S. A., Koffi, B., Myhre, G., Olivié, D., Prather, M. J., Pyle, J. A., Stordal, F., Szopa, S., Tang, Q., van Velthoven, P., Williams, J. E., & Ødemark, K. (2011). Future impact of non-land based traffic emissions on atmospheric ozone and OH – an optimistic scenario and a possible mitigation strategy. *Atmospheric Chemistry and Physics*, 11(21), 11293–11317. <https://doi.org/10.5194/acp-11-11293-2011>
- 460 Hodnebrog, Ø., Berntsen, T. K., Dessens, O., Gauss, M., Grewe, V., Isaksen, I. S. A., Koffi, B., Myhre, G., Olivié, D., Prather, M. J., Stordal, F., Szopa, S., Tang, Q., van Velthoven, P., & Williams, J. E. (2012). Future impact of traffic emissions on atmospheric ozone and OH based on two scenarios. *Atmospheric Chemistry and Physics*, 12(24), 12211–12225. <https://doi.org/10.5194/acp-12-12211-2012>
- Hoesly, R. M., Smith, S. J., Feng, L., Klimont, Z., Janssens-Maenhout, G., Pitkanen, T., Seibert, J. J., Vu, L., Andres, R. J., Bolt, R. M., Bond, T. C., Dawidowski, L., Kholod, N., Kurokawa, J., Li, M., Liu, L., Lu, Z., Moura, M. C. P., O'Rourke, P. R., & Zhang, Q. (2018). Historical (1750–2014) anthropogenic emissions of reactive gases and aerosols



from the Community Emissions Data System (CEDs). *Geoscientific Model Development*, 11(1), 369–408.

<https://doi.org/10.5194/gmd-11-369-2018>

470 Holmes, C. D., Tang, Q., & Prather, M. J. (2011). Uncertainties in climate assessment for the case of aviation NO. *Proceedings of the National Academy of Sciences*, 108(27), 10997–11002. <https://doi.org/10.1073/pnas.1101458108>

ICAO. (2025, June 1). *ICAO Environmental Report 2025*. <https://www.icao.int/environmental-protection/Pages/envrep2025.aspx>

IEA. (2025). *Aviation*. IEA. <https://www.iea.org/energy-system/transport/aviation>

475 Khodayari, A., Vitt, F., Phoenix, D., & Wuebbles, D. J. (2018). The impact of NO<sub>x</sub> emissions from lightning on the production of aviation-induced ozone. *Atmospheric Environment*, 187, 410–416. <https://doi.org/10.1016/j.atmosenv.2018.05.057>

Kinnison, D. E., Brasseur, G. P., Walters, S., Garcia, R. R., Marsh, D. R., Sassi, F., Harvey, V. L., Randall, C. E., Emmons, L., Lamarque, J. F., Hess, P., Orlando, J. J., Tie, X. X., Randel, W., Pan, L. L., Gettelman, A., Granier, C., Diehl, T., Niemeier, U., & Simmons, A. J. (2007). Sensitivity of chemical tracers to meteorological parameters in the MOZART-3 chemical transport model. *Journal of Geophysical Research: Atmospheres*, 112(D20).  
 480 <https://doi.org/10.1029/2006JD007879>

Klöwer, M., Allen, M. R., Lee, D. S., Proud, S. R., Gallagher, L., & Skowron, A. (2021). Quantifying aviation’s contribution to global warming. *Environmental Research Letters*, 16(10), 104027. <https://doi.org/10.1088/1748-9326/ac286e>

Köhler, M. O., Rädcl, G., Dessens, O., Shine, K. P., Rogers, H. L., Wild, O., & Pyle, J. A. (2008a). Impact of perturbations to nitrogen oxide emissions from global aviation. *Journal of Geophysical Research: Atmospheres*, 113(D11).  
 485 <https://doi.org/10.1029/2007JD009140>

Köhler, M. O., Rädcl, G., Dessens, O., Shine, K. P., Rogers, H. L., Wild, O., & Pyle, J. A. (2008b). Impact of perturbations to nitrogen oxide emissions from global aviation. *Journal of Geophysical Research: Atmospheres*, 113(D11).  
<https://doi.org/10.1029/2007JD009140>

Lee, D. S., Fahey, D. W., Skowron, A., Allen, M. R., Burkhardt, U., Chen, Q., Doherty, S. J., Freeman, S., Forster, P. M.,  
 490 Fuglestedt, J., Gettelman, A., De León, R. R., Lim, L. L., Lund, M. T., Millar, R. J., Owen, B., Penner, J. E., Pitari,



- G., Prather, M. J., ... Wilcox, L. J. (2021). The contribution of global aviation to anthropogenic climate forcing for 2000 to 2018. *Atmospheric Environment*, 244, 117834. <https://doi.org/10.1016/j.atmosenv.2020.117834>
- Liu, M., Song, Y., Matsui, H., Shang, F., Kang, L., Cai, X., Zhang, H., & Zhu, T. (2024). Enhanced atmospheric oxidation toward carbon neutrality reduces methane's climate forcing. *Nature Communications*, 15(1), 3148. <https://doi.org/10.1038/s41467-024-47436-9>
- 495 Lund, M. T., Aamaas, B., Berntsen, T., Bock, L., Burkhardt, U., Fuglestad, J. S., & Shine, K. P. (2017). Emission metrics for quantifying regional climate impacts of aviation. *Earth System Dynamics*, 8(3), 547–563. <https://doi.org/10.5194/esd-8-547-2017>
- Lund, M. T., Rap, A., Myhre, G., Haslerud, A. S., & Samset, B. H. (2021). Land cover change in low-warming scenarios may enhance the climate role of secondary organic aerosols. *Environmental Research Letters*, 16(10), 104031. <https://doi.org/10.1088/1748-9326/ac269a>
- 500 Maruhashi, J., Mertens, M., Grewe, V., & Dedoussi, I. C. (2024). A multi-method assessment of the regional sensitivities between flight altitude and short-term O3 climate warming from aircraft NOx emissions. *Environmental Research Letters*, 19(5), 054007. <https://doi.org/10.1088/1748-9326/ad376a>
- 505 Myhre, G., Shine, K. P., Rädel, G., Gauss, M., Isaksen, I. S. A., Tang, Q., Prather, M. J., Williams, J. E., van Velthoven, P., Dessens, O., Koffi, B., Szopa, S., Hoor, P., Grewe, V., Borken-Kleefeld, J., Berntsen, T. K., & Fuglestad, J. S. (2011). Radiative forcing due to changes in ozone and methane caused by the transport sector. *Atmospheric Environment*, 45(2), 387–394. <https://doi.org/10.1016/j.atmosenv.2010.10.001>
- Olsen, S. C., Brasseur, G. P., Wuebbles, D. J., Barrett, S. R. H., Dang, H., Eastham, S. D., Jacobson, M. Z., Khodayari, A., Selkirk, H., Sokolov, A., & Unger, N. (2013). Comparison of model estimates of the effects of aviation emissions on atmospheric ozone and methane. *Geophysical Research Letters*, 40(22), 6004–6009. <https://doi.org/10.1002/2013GL057660>
- 510 O'Neill, B. C., Tebaldi, C., van Vuuren, D. P., Eyring, V., Friedlingstein, P., Hurtt, G., Knutti, R., Kriegler, E., Lamarque, J.-F., Lowe, J., Meehl, G. A., Moss, R., Riahi, K., & Sanderson, B. M. (2016). The Scenario Model Intercomparison



- 515 Project (ScenarioMIP) for CMIP6. *Geoscientific Model Development*, 9(9), 3461–3482. <https://doi.org/10.5194/gmd-9-3461-2016>
- Petzold, A., Thouret, V., Gerbig, C., Zahn, A., Brenninkmeijer, C. A. M., Gallagher, M., Hermann, M., Pontaud, M., Ziereis, H., Boulanger, D., Marshall, J., Nédélec, P., Smit, H. G. J., Friess, U., Flaud, J.-M., Wahner, A., Cammas, J.-P., & Volz-Thomas, A. (2015). Global-scale atmosphere monitoring by in-service aircraft – current achievements and  
 520 future prospects of the European Research Infrastructure IAGOS. *Tellus B: Chemical and Physical Meteorology*, 67(1), 28452. <https://doi.org/10.3402/tellusb.v67.28452>
- Ponater, M., Pechtl, S., Sausen, R., Schumann, U., & Hüttig, G. (2006). Potential of the cryoplane technology to reduce aircraft climate impact: A state-of-the-art assessment. *Atmospheric Environment*, 40(36), 6928–6944. <https://doi.org/10.1016/j.atmosenv.2006.06.036>
- 525 Pozzer, A., Jöckel, P., Kern, B., & Haak, H. (2011). The Atmosphere-Ocean General Circulation Model EMAC-MPIOM. *Geoscientific Model Development*, 4(3), 771–784. <https://doi.org/10.5194/gmd-4-771-2011>
- Prashanth, P., Eastham, S. D., Speth, R. L., & Barrett, S. R. H. (2022). Aerosol formation pathways from aviation emissions. *Environmental Research Communications*, 4(2), 021002. <https://doi.org/10.1088/2515-7620/ac5229>
- Righi, M., Hendricks, J., & Beer, C. G. (2021). Exploring the uncertainties in the aviation soot–cirrus effect. *Atmospheric  
 530 Chemistry and Physics*, 21(23), 17267–17289. <https://doi.org/10.5194/acp-21-17267-2021>
- Sand, M., Skeie, R. B., Sandstad, M., Krishnan, S., Myhre, G., Bryant, H., Derwent, R., Hauglustaine, D., Paulot, F., Prather, M., & Stevenson, D. (2023). A multi-model assessment of the Global Warming Potential of hydrogen. *Communications Earth & Environment*, 4(1), 1–12. <https://doi.org/10.1038/s43247-023-00857-8>
- Skeie, R. B., Myhre, G., Hodnebrog, Ø., Cameron-Smith, P. J., Deushi, M., Hegglin, M. I., Horowitz, L. W., Kramer, R. J.,  
 535 Michou, M., Mills, M. J., Olivié, D. J. L., Connor, F. M. O., Paynter, D., Samset, B. H., Sellar, A., Shindell, D., Takemura, T., Tilmes, S., & Wu, T. (2020). Historical total ozone radiative forcing derived from CMIP6 simulations. *Npj Climate and Atmospheric Science*, 3(1), Article 1. <https://doi.org/10.1038/s41612-020-00131-0>





- Skowron, A., Lee, D. S., De León, R. R., Lim, L. L., & Owen, B. (2021). Greater fuel efficiency is potentially preferable to reducing NO<sub>x</sub> emissions for aviation's climate impacts. *Nature Communications*, 12(1), Article 1.  
 540 <https://doi.org/10.1038/s41467-020-20771-3>
- Søvde, O. A., Matthes, S., Skowron, A., Iachetti, D., Lim, L., Owen, B., Hodnebrog, Ø., Di Genova, G., Pitari, G., Lee, D. S., Myhre, G., & Isaksen, I. S. A. (2014). Aircraft emission mitigation by changing route altitude: A multi-model estimate of aircraft NO<sub>x</sub> emission impact on O<sub>3</sub> photochemistry. *Atmospheric Environment*, 95, 468–479.  
<https://doi.org/10.1016/j.atmosenv.2014.06.049>
- 545 Søvde, O. A., Prather, M. J., Isaksen, I. S. A., Berntsen, T. K., Stordal, F., Zhu, X., Holmes, C. D., & Hsu, J. (2012). The chemical transport model Oslo CTM3. *Geoscientific Model Development*, 5(6), 1441–1469.  
<https://doi.org/10.5194/gmd-5-1441-2012>
- Stevenson, D. S., & Derwent, R. G. (2009). Does the location of aircraft nitrogen oxide emissions affect their climate impact? *Geophysical Research Letters*, 36(17). <https://doi.org/10.1029/2009GL039422>
- 550 Terrenoire, E., Hauglustaine, D. A., Cohen, Y., Cozic, A., Valorso, R., Lefèvre, F., & Matthes, S. (2022). Impact of present and future aircraft NO<sub>x</sub> and aerosol emissions on atmospheric composition and associated direct radiative forcing of climate. *Atmospheric Chemistry and Physics*, 22(18), 11987–12023. <https://doi.org/10.5194/acp-22-11987-2022>
- Thor, R. N., Mertens, M., Matthes, S., Righi, M., Hendricks, J., Brinkop, S., Graf, P., Grewe, V., Jöckel, P., & Smith, S. (2023). An inconsistency in aviation emissions between CMIP5 and CMIP6 and the implications for short-lived species and  
 555 their radiative forcing. *Geoscientific Model Development*, 16(5), 1459–1466. <https://doi.org/10.5194/gmd-16-1459-2023>
- Unger, N., Zhao, Y., & Dang, H. (2013). Mid-21st century chemical forcing of climate by the civil aviation sector. *Geophysical Research Letters*, 40(3), 641–645. <https://doi.org/10.1002/grl.50161>
- van Vuuren, D. P., Stehfest, E., Gernaat, D. E. H. J., Doelman, J. C., van den Berg, M., Harmsen, M., de Boer, H. S., Bouwman, L. F., Daioglou, V., Edelenbosch, O. Y., Girod, B., Kram, T., Lassaletta, L., Lucas, P. L., van Meijl, H., Müller, C.,  
 560 van Ruijven, B. J., van der Sluis, S., & Tabeau, A. (2017). Energy, land-use and greenhouse gas emissions trajectories



under a green growth paradigm. *Global Environmental Change*, 42, 237–250.

<https://doi.org/10.1016/j.gloenvcha.2016.05.008>